

# Constituent quark scaling violation due to baryon number transport

J.C. Dunlop,<sup>1</sup> M.A. Lisa,<sup>2</sup> and P. Sorensen<sup>1</sup>

<sup>1</sup>*Brookhaven National Laboratory, Upton New York 11973, USA*

<sup>2</sup>*Department of Physics, Ohio State University, Columbus, Ohio 43210, USA*

In ultra-relativistic heavy ion collisions at  $\sqrt{s_{NN}} \approx 200$  GeV, the azimuthal emission anisotropy of hadrons with low and intermediate transverse momentum ( $p_T \lesssim 4$  GeV/c) displays an intriguing scaling. In particular, the baryon (meson) emission patterns are consistent with a scenario in which a bulk medium of flowing quarks coalesces into three-quark (two-quark) “bags.” While a full understanding of this number of constituent quark (NCQ) scaling remains elusive, it is suggestive of a thermalized bulk system characterized by colored dynamical degrees of freedom— a quark-gluon plasma (QGP). In this scenario, one expects the scaling to break down as the central energy density is reduced below the QGP formation threshold; for this reason, NCQ-scaling violation searches are of interest in the energy scan program at the Relativistic Heavy Ion Collider (RHIC). However, as  $\sqrt{s_{NN}}$  is reduced, it is not only the initial energy density that changes; there is also an increase in the net baryon number at midrapidity, as stopping transports entrance-channel partons to midrapidity. This phenomenon can result in violations of simple NCQ scaling. Still in the context of the quark coalescence model, we describe a specific pattern for the break-down of the scaling that includes different flow strengths for particles and their anti-partners. Related complications in the search for recently suggested exotic phenomena are also discussed.

PACS numbers: 25.75.-q, 25.75.Gz, 25.70.Pq

Keywords: quark-gluon plasma, constituent quark scaling, stopping, heavy ions

## I. INTRODUCTION

### A. Quark coalescence in the highest-energy heavy ion collisions

Hadronization— the process through which a state characterized by colored dynamical partons is resolved into a state of colorless hadrons— is central to the theory of the Strong interaction, but remains only incompletely understood. An important aspect of this process has become clear in studies of the forward region in hadron-hadron collisions [1] and in high-multiplicity collisions of ultra-relativistic heavy ion collisions [2, 3]: the hadronization of a parton is strongly affected by the presence of other partons close in phase space. Whereas the vacuum hadronization of a single parton liberated in a high momentum-transfer ( $Q^2$ ) interaction is described in terms of string-breaking scenarios or parameterized in fragmentation functions, there is mounting evidence that, in a dense phase-space scenario, colored partons essentially “coalesce” into colorless bound states, much like the formation of light nuclei (e.g. deuteron or triton) from free nucleons emitted from a hot zone [4–6]. Models based on this remarkably simple mechanism, not understood at a fundamental level, have enjoyed considerable success at describing the “leading hadron effect” [7] as well as the multiplicity dependence of yields, spectra and momentum anisotropies from heavy ion collisions at the highest energies at the Relativistic Heavy Ion Collider (RHIC) [8–12].

Even more remarkably, the objects that coalesce appear to be valence quarks. At first, this is surprising, since the dynamical quantities in QCD (i.e. the ones that carry momentum) are *partons* which are overwhelmingly gluons and

non-valence quarks. Indeed, the valence *quarks*<sup>1</sup>— three for baryons and two for mesons— were originally invented to explain the flavored quantum numbers— isospin, strangeness, etc— of the hadrons. Only later was the connection established between the valence quarks and the high momentum-fraction ( $x$ ) fermionic partons. Nevertheless, the two or three valence quarks represent the lowest Fock states of the partonic wavefunction of a hadron, and these appear the relevant degrees of freedom; it is argued that inclusion of higher-order Fock states does not significantly modify the description of the coalescence process and the related phenomenology [13].

The data at RHIC is consistent with a partially thermalized system of deconfined quarks undergoing collective expansion with an azimuthal anisotropy in momentum space proportional to the initial spatial anisotropy [3, 14, 15]. As the system cools, pairs and triplets of neighboring quarks coalesce to become the valence quarks (or “constituent quarks”) of mesons and baryons (where the gluons presumably contribute to dressing the valence quarks [16, 17]). The original flow pattern of the deconfined quarks leaves a simple and characteristic fingerprint on the momentum distribution of the observed hadrons, since a hadron’s momentum is simply the (vector) sum of the momenta of its valence quarks

$$\vec{p}_h = \sum_{i=1}^n \vec{p}_{q,i}, \quad (1)$$

where  $n = 2$  (3) for mesons (baryons). In the simplest instantaneous  $2 \rightarrow 1$  or  $3 \rightarrow 1$  coalescence process, only three of the four momentum components are conserved; either energy or momentum conservation is violated [12]. The most important

<sup>1</sup> Anti-quarks are treated on equal footing with quarks in coalescence models. Dynamically, we will treat antiquarks as simply another variety of quark.

features of quark coalescence that we discuss in this paper are not substantially altered in a more complete treatment of the phenomenon, accounting for energy and entropy conservation effects [12, 18, 19].

In particular, the quarks' radial flow— the enhancement towards higher transverse momentum ( $p_T$ ) due to pressure-driven expansion of the bulk source— is reflected most strongly in the three-quark baryons. Thus, coalescence provides a natural explanation for the “anomalous baryon enhancement” at intermediate  $p_T$  observed in the highest-energy heavy ion collisions at RHIC [2]. Similarly, the nuclear modification factor— the scaled ratio  $R_{AA}(p_T)$  of transverse momentum distributions from heavy ion and  $p + p$  collisions— shows a clear separation into mesons and baryons [3, 15].

In heavy ion collisions, the azimuthal anisotropy of the momentum distribution is characterized by Fourier components,

$$\frac{dN}{d\phi} \propto 1 + 2 \sum_{n=1} v_n(p_T) \cos n\phi, \quad (2)$$

where  $\phi$  is measured relative to the direction of the impact parameter [c.f. 20, for a full discussion]. Of particular interest is the elliptic flow parameter  $v_2(p_T)$ , which is strongly sensitive to the equation of state of QCD matter (e.g. speed of sound) as well as transport coefficients like viscosity. For small values of  $v_2$  and narrow hadronic wavefunctions, the elliptic flow parameters of a bulk system of quarks ( $a$  and  $b$ ) and the mesons into which they coalesce, are related by [12]

$$v_2^M(p_T) = v_2^a(x_a p_T) + v_2^b(x_b p_T) \quad (3)$$

for fixed momentum fractions  $x_a$  and  $x_b$  ( $x_a + x_b = 1$ ), with an analogous equation for baryons.

In the event that the constituent quarks ( $a$  and  $b$ ) have the same elliptic flow before hadronization, Equation 3 leads to the number-of-constituent-quark (NCQ) scaling pattern observed at RHIC,

$$v_2^h(p_T^h) = n v_2^q(p_T^h/n), \quad (4)$$

where  $n = 2$  (3) for mesons (baryons). In this scenario, all mesons should follow one common  $v_2(p_T)$  curve, and all baryons another. The two should be related via

$$\frac{v_2^B(p_T/3)}{3} = \frac{v_2^M(p_T/2)}{2} \quad (= v_2^q(p_T)). \quad (5)$$

## B. Violation of NCQ scaling

The observed satisfaction of Eq. 5 in Au+Au collisions at RHIC was one of the most compelling indications that deconfined partonic degrees of freedom were playing a dynamic role in the bulk medium of the early phase. Consequently, the *breakdown* of this scaling as the beam energy is reduced, is an important signal in the RHIC energy scan program [21]. It may indicate that the initial energy density of the system is below the threshold for QGP creation, pinpointing the phase transition between confined and deconfined QCD matter.

Additionally, it has been recently proposed [22] that a deconfined bulk system at finite baryon density may acquire an electric quadrupole moment due to chiral magnetic waves in the plasma. This interesting phenomenon would break the degeneracy between  $v_2$  for positive and negative pions, also clearly breaking NCQ scaling.

It is important to consider other less exotic mechanisms that may also cause violation of the scaling represented by Eq. 5. In particular, we recall that this scaling should hold if all quarks (and antiquarks) have the same underlying flow distribution ( $v_2^q$  in equation 5). This would be a natural consequence of thermalization. The scenario where all constituent quarks have the same  $v_2^q$  we call NCQ<sub>1</sub>.

In this paper, we examine whether the breakdown of Eq. 5 would necessarily signal that the hadrons are not resulting from the coalescence of flowing constituent quarks. In particular, we discuss a minimal extension of the NCQ<sub>1</sub> model that retains constituent quarks as the dynamical degrees of freedom and coalescence as the hadronization mechanism. However, the assumption that all quarks have the same  $v_2^q$  is discarded due to the well-recognized phenomenon of baryon stopping, which is increasingly important at lower energies. In particular, we recall that the transport of baryon number from the entrance channel to midrapidity (“stopping”) is increasingly important at lower energies. Since we continue to work in the dynamical constituent quark paradigm, this means that  $u$  and  $d$  quarks transported from  $y = y_{\text{beam}}$  to  $y = 0$  surely suffer multiple collisions with each other. Meanwhile, at the lower energies in question, the quark-antiquark pairs created from the vacuum may experience relatively fewer. In a picture where  $v_2^q$  is developed through collisions, it is not unreasonable to expect that quarks transported from  $y = y_{\text{beam}}$  to  $y = 0$  will develop a larger  $v_2$ .

Such considerations will lead to a specific pattern for the breakdown of Eq. 5. Without invoking exotic phenomena, this simple scenario also implies that the degeneracy of  $v_2$  for particles and their anti-partners will be broken in a specific way. Not only its prediction for  $v_2[\pi^+] - v_2[\pi^-]$ , but also that for  $v_2[K^+] - v_2[K^-]$ , can be compared to data and predictions from more complicated models.

In the following section, we briefly review the energy dependence of stopping in heavy ion collisions— transport of baryon number from the high-rapidity region of the entrance channel to midrapidity in the exit channel. We also use measured particle yields to estimate the fraction of  $u$  and  $d$  quarks at midrapidity that would arise from baryon stopping at two collision energies. In section III, we consider quantitatively a two component model for quark number scaling NCQ<sub>2</sub>, in which the phenomenon of stopping leads to at least two samples of quarks with different  $v_2^q$  values which then coalesce into hadrons. For tractability, we idealize this non-thermal distribution in a two-component formalism: transported quarks follow one flow profile and produced quarks another. We briefly summarize in section IV.

## II. TRANSPORT OF ENTRANCE-CHANNEL QUARKS TO MIDRAPIDITY

In this section, we briefly review the phenomenon of baryon stopping in heavy ion collisions. We then use hadron yields measured by the NA49/SPS collaboration to estimate the fraction of  $u$  and  $d$  quarks at midrapidity that would arise from stopping. These fractions will be used in section III as input to a simple model to predict the breakdown of NCQ scaling, Eq. 5.

### A. Stopping in heavy ion collisions

In the RHIC energy scan program, the beam energy is varied to modify the initial conditions of the hot QCD system created. In addition to changing the energy density of the initial state, it is well-accepted that, due to baryon stopping, the baryo-chemical potential  $\mu_B$  of the system is larger at lower  $\sqrt{s_{NN}}$ .

Baryon stopping, the transport of baryon number from its initial location at beam rapidity towards the initially baryon-free region at mid-rapidity, is most directly measured via the rapidity distribution of net protons (the number of protons minus antiprotons). At  $\sqrt{s_{NN}} \approx 5$  GeV, the rapidity distribution is peaked at midrapidity. As the collision energy is increased, the distribution peaks at increasingly forward rapidity. This behavior has been parametrized as an average rapidity loss, which increases from approximately 1 unit at  $\sqrt{s_{NN}} \approx 5$  GeV to 1.7 unit at  $\sqrt{s_{NN}} \approx 17$  GeV, with a smaller rise towards 2 units by the highest RHIC  $\sqrt{s_{NN}}$  of 200 GeV[23]. This rise in rapidity loss is less rapid than the rise in the beam rapidity with increasing  $\sqrt{s_{NN}}$ , leading to a decreasing population of net baryon number at mid-rapidity.

More detailed statistical model calculations, based on measurements of the yields of a range of particles, agree with this general conclusion. Within these models, with increasing  $\sqrt{s_{NN}}$  the net baryon density first rises, achieves a maximum at  $\sqrt{s_{NN}} \approx 8$  GeV, and then falls for higher  $\sqrt{s_{NN}}$  [24]. The system transitions from one with entropy density dominated by baryons at low energy to one dominated by mesons at high energy, with equal fractions at  $\sqrt{s_{NN}} \approx 8$  GeV [25]. The *fractional* importance of transported quarks to the system's evolution grows rapidly with decreasing  $\sqrt{s_{NN}}$  in the lower end of the region probed by the RHIC Beam Energy scan, from  $\sqrt{s_{NN}} \approx 15$  GeV to 7.7 GeV.

### B. Estimates for the stopping contribution to light quark yields at midrapidity

In section III, we develop a simple model in which transported  $u$  and  $d$  quarks have stronger flow than do produced quarks (including produced  $u$  and  $d$  quarks). An important ingredient to this model is the fraction of  $u$  ( $d$ ) quarks present at midrapidity that arise from baryon number transport. In

hadron	yield	$u$	$d$	$s$	$\bar{u}$	$\bar{d}$	$\bar{s}$
$\pi^+$	72.9	72.9				72.9	
$\pi^-$	84.8		84.8		84.8		
$\pi^0$ (*)	78.85	39.43	39.43		39.43	39.43	
$\phi$	1.17			1.17			1.17
$K^+$	16.4	16.4					16.4
$K^-$	5.58			5.58	5.58		
$K^0$ (*)	10.99		10.99				13.84
$\bar{K}^0$ (*)	10.99			10.99		10.99	
p	46.1	92.2	46.1				
n (*)	70.84	70.84	141.68				
$\Lambda$	13.4	13.4	13.4	13.4			
$\Xi^-$	0.93		0.93	1.86			
$\bar{p}$	0.06				0.12	0.06	
$\bar{n}$ (*)	0.04				0.04	0.08	
$\bar{\Lambda}$	0.1				0.1	0.1	0.1
Sum		305.17	337.33	33	130.07	123.56	28.66

TABLE I: Left two columns: midrapidity yields of common particles from central Pb+Pb collisions measured by the NA49/SPS Collaboration [26–33] at  $\sqrt{s_{NN}} = 6.41$  GeV. Starred hadrons are not measured, but estimated from other hadrons. In particular,  $dN[\pi^0]/dy = 0.5(dN[\pi^+]/dy + dN[\pi^-]/dy)$ ,  $dN[K^0]/dy = dN[\bar{K}^0]/dy = 0.5(dN[K^+]/dy + dN[K^-]/dy)$ ,  $dN[n] = 1.54dN[p]$ , and  $dN[\bar{n}] = 1.54^{-1}dN[\bar{p}]$ . The factor 1.54 is the neutron-to-proton ratio of Pb. Right six columns: midrapidity yield of constituent quarks for each hadron.

particular, we want the fraction

$$X_{uT} \equiv \frac{N_{uT}}{N_{uT} + N_{uP}}, \quad (6)$$

where  $N_{uT}$  is the number of  $u$  quarks from the incoming heavy ions transported to midrapidity, and  $N_{uP}$  is the number of  $u$  quarks produced from  $u - \bar{u}$  pair production at midrapidity. The fraction  $X_{dT}$  is defined similarly.

To estimate  $X_{uT}$  and  $X_{dT}$ , we use measured midrapidity yields of common particles from central Pb+Pb collisions by the NA49/SPS Collaboration at  $\sqrt{s_{NN}} = 6.41$  and 8.86 GeV. Tables I and II list the measured yields of hadrons and their constituent quarks.

Since produced quarks and antiquarks are formed in pairs, the number of transported  $u$  quarks is given by the imbalance between the total number of  $u$  and  $\bar{u}$  quarks;  $X_{uT} = (N_u - N_{\bar{u}})/N_u$ . Table III lists the fractions for the two energies.

Several comments are in order. Firstly, at these energies, roughly half of the light constituent quarks at midrapidity originate from the colliding nuclei; clearly stopping cannot be ignored. Secondly, the fraction of  $d$  quarks transported from the  $y = y_{\text{beam}}$  is greater than the fraction of  $u$  quarks, simply as a consequence of the isospin of the entrance channel. Thirdly, the imbalance in  $s$  and  $\bar{s}$  quarks in tables I and II reminds us that our estimates are just that.

hadron	yield	$u$	$d$	$s$	$\bar{u}$	$\bar{d}$	$\bar{s}$
$\pi^+$	96.6	96.6				96.6	
$\pi^-$	106.1		106.1		106.1		
$\pi^0$ (*)	101.35	50.68	50.68		50.68	50.68	
$\phi$	1.16			1.16			1.16
$K^+$	20.1	20.1					20.1
$K^-$	7.58			7.58	7.58		
$K^0$ (*)	13.84		13.84				13.84
$\bar{K}^0$ (*)	13.84			13.84		13.84	
$p$	41.3	82.6	41.3				
$n$ (*)	63.5	63.5	127				
$d$	1.02	3.06	3.06	3.06			
$\Lambda$	14.6	14.6	14.6	14.6			
$\Xi^-$	1.15		1.15	2.3			
$\bar{p}$	0.32				0.64	0.32	
$\bar{n}$ (*)	0.21				0.21	0.42	
$\bar{\Lambda}$	0.33				0.33	0.33	0.33
$\Xi^+$	0.07					0.07	0.14
Sum		331.14	357.73	39.48	165.54	162.26	35.57

TABLE II: The same as for table I, but for  $\sqrt{s_{NN}} = 8.86$  GeV collisions.

$\sqrt{s_{NN}}$	$X_{u^T}$	$X_{d^T}$
6.41 GeV	0.57	0.63
8.86 GeV	0.50	0.55

TABLE III: Based on the data in tables I and II, the fraction of  $u$  and  $d$  quarks at midrapidity, that originate from stopping of quarks in the colliding Pb nuclei. See text for details.

### III. VIOLATIONS OF SIMPLE NCQ SCALING IN A TWO-COMPONENT SCENARIO

As discussed in section I, the violation of NCQ scaling, eq. 5 and the breakdown of the degeneracy of  $v_2$  between particles and antiparticles, implies a lack of kinetic thermalization of the dynamic system. This may arise if the energy of the collision falls below the threshold to produce a flowing system of deconfined partons, so that particle-specific hadronic cross-sections determine each hadron's flow strength. Alternatively, it may arise from more interesting phenomena such as chiral magnetic waves. Our approach in this paper is a minimalist one, asking whether such effects may be expected without invoking exotic phenomena or abandoning a scenario of flowing quarks which coalesce into flowing hadrons.

The absence of complete kinetic thermalization at low energies ( $\sqrt{s_{NN}} \lesssim 30$  GeV) has long been recognized, based on the severe failure of hydrodynamics to reproduce hadronic  $v_2$  [34]. In short, at these energies, the constituents of the system do not rescatter sufficiently to achieve thermalization. As we have discussed, at these energies baryon transport from the entrance channel plays a huge role. We wish to test the robustness of the constituent quark paradigm, so the transported baryon number is represented by transported  $u$  and  $d$  quarks.

The very fact that they have been transported over a significant rapidity range attests to the likelihood that these quarks, in any event, have suffered many scatterings. We make the plausible postulate that transported quarks experience more scatterings than produced ones at these energies, hence approaching the thermal limit more closely and developing a larger  $v_2$ .

Clearly, the resulting non-thermal quark momentum distribution reflects a continuum of quarks rescattering more or less before coalescence. In order to render the problem tractable, we model the situation in a simple limit of two populations: transported quarks and produced quarks, with the former population characterized by a stronger flow than the latter. We emphasize that this is a simplification in order to make a point: we do not propose that there are really two distinct thermalized fluids created in a heavy ion collision.

Hence, we have two populations of constituent quarks with distinct flow fields,  $v_2^{q^P}$  and  $v_2^{q^T}$ , for produced ( $u^P, \bar{u}^P, d^P, \bar{d}^P, s^P, \bar{s}^P$ ) and transported ( $u^T, \bar{d}^T$ ) quarks, respectively. In this simplest two-component model, a hadron's elliptic flow parameter is given by

$$v_2^h(p_T) = \sum_{i=1}^n \left[ X_{q_i^T} v_2^{q_i^T}(p_T/n) + (1 - X_{q_i^T}) v_2^{q_i^P}(p_T/n) \right], \quad (7)$$

where  $X_{q_i^T}$  is the fraction of quark species  $q_i$  that originates from baryon stopping, as discussed in section II. As per the discussion in that section, reasonable estimates are  $X_u = 0.50$  and  $X_d = 0.55$ . Naturally,  $X_{\bar{u}^T} = X_{\bar{d}^T} = X_{s^T} = X_{\bar{s}^T} = 0$ .

Figure 1 shows a example of the resulting  $v_2$  from our simple NCQ<sub>2</sub> scenario. For the purpose of illustration, for these calculations, we had to assume some functional form for the quark elliptic flow. We chose the same functional form for both produced and transported quarks:

$$v_2(p_T) = M \tanh(p_T / (0.5 \text{ GeV}/c)). \quad (8)$$

For the example in figure 1,  $M = 0.07$  for transported quarks and  $M = 0.05$  for produced quarks. The choice of this particular functional form is rather arbitrary and does not affect the points we make below.

Clearly, simple NCQ scaling (equation 5) is violated, with an unavoidable species-dependent signature. In particular, one finds:

$$\begin{aligned} v_2[\pi^- = d\bar{u}] &> v_2[\pi^+ = u\bar{d}] \\ v_2[K^+ = u\bar{s}] &> v_2[K^- = \bar{u}s] \\ v_2[p = uud] &> v_2[\bar{p} = \bar{u}\bar{u}\bar{d}] \\ v_2[\Lambda = uds] &> v_2[\bar{\Lambda} = \bar{u}\bar{d}\bar{s}] \\ v_2[p = uud] &> v_2[\Lambda = uds] \end{aligned} \quad (9)$$

$$(v_2[p = uud] - v_2[\bar{p} = \bar{u}\bar{u}\bar{d}]) > (v_2[\Lambda = uds] - v_2[\bar{\Lambda} = \bar{u}\bar{d}\bar{s}]).$$

It is interesting that the ordering of  $v_2$  for positive and negative pions is the same as that predicted due to chiral magnetic wave effects [22]. We also find that the charge-ordering for kaons ( $v_2[K^+] > v_2[K^-]$ ) is opposite to that for pions. The chiral magnetic wave effect would generate the *same* charge-ordering for pions as for kaons, thus providing a testable distinction between the chiral magnetic model and our stopping-based model. However, hadronic effects (e.g. the smaller

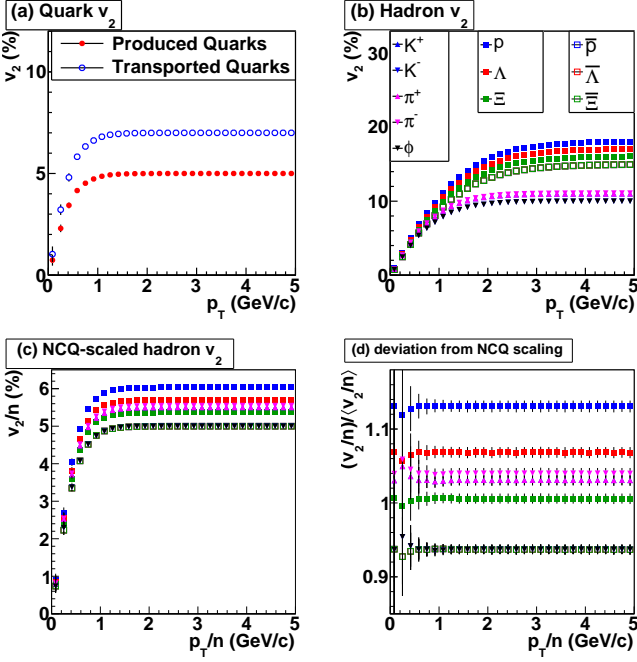


FIG. 1: (Color online) NCQ<sub>2</sub>, the simplest generalization of the NCQ<sub>1</sub> model, in which the transported up and down quarks have a 40% stronger intrinsic  $v_2$  than do the produced quarks, which themselves all have the same  $v_2$ . The fraction of  $u$  and  $d$  quarks that are transported is 50% and 55%, respectively. See text for details.

Panel (a): Intrinsic  $v_2$  of all quarks.

Panel (b): Hadron  $v_2$  based on coalescence of quarks shown to the left.

Panel (c): NCQ-scaled hadron flow,  $v_2(p_T/n)/n$ .

Panel (d): Deviation from simple NCQ scaling— the curves from the lower left panel, divided by their average.

In panels (b)-(d),  $K^+$  data points lie beneath those for  $\pi^+$ ,  $K^-$  data points lie beneath those of  $\phi$ , and the data points for all anti-baryons are coincident.

cross-section for  $K^-$ ) may complicate the interpretation of such a test [35].

Comparing the anisotropies of particles and their anti-partners, as listed in equation 9, is straightforward and relatively unambiguous. The details of cross-species comparisons can depend more on the particular functional forms used for the quark flow profiles, the weighting factors  $X_{q_i}$  and whether the latter depend on  $p_T$ . For the simple case we have considered,  $\frac{v_2[p]}{3} > \frac{v_2[\pi^\pm]}{2}$ ; the entire species dependences can be seen in panels (d) of figures 1 and 2.

Our primary points have been made already in this simple model, but we mention an additional complication. If there is insufficient rescattering to fully thermalize the light produced quarks, then the heavier strange produced quarks are likely to be even less thermalized. In this case,  $v_2^P < v_2^{uP,dP}$ ; similar considerations have been discussed by Lin and Ko [36]. Figure 2 shows the situation when the functional form of equation 8 describes the flow of all quarks, as before, but now  $M=0.045$  for the strange quarks. In this case, the degeneracies

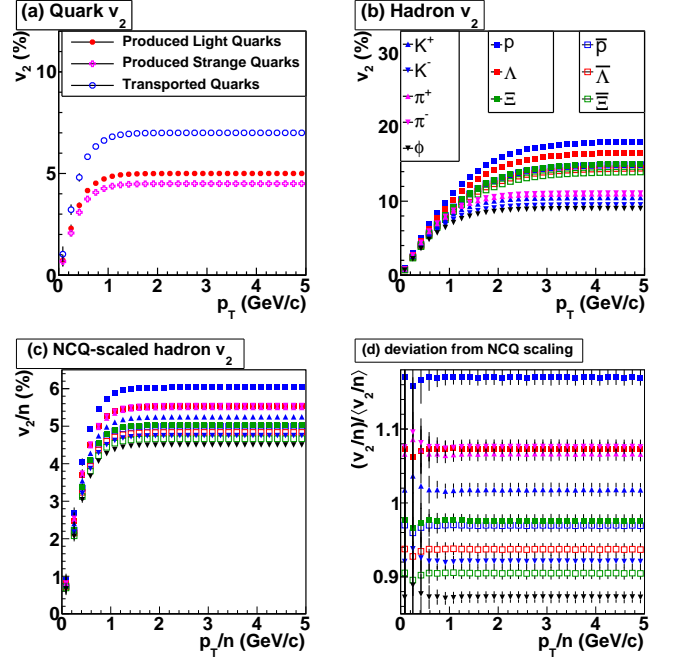


FIG. 2: (Color online) The same as in figure 1, but the produced strange quarks have 10% less intrinsic  $v_2$  than do the produced light quarks. See text for details.

(e.g.  $v_2[K^-] = v_2[\phi]$ ) seen in figure 1 and listed in its caption are broken; all hadrons have distinct elliptic flow curves.

Additional reasonable complications can be considered. Clearly, the functional forms used for the quark flow can be varied from the simple form (eq. 8) used here. Furthermore, one may reasonably argue that the fraction of light quarks arising from transport ( $X_{q_i}$ ) should depend on  $p_T$ ; we have treated it as a constant for simplicity. Exploring such considerations amounts to tuning the model. We leave such explorations for later comparison and fitting when data become available.

#### IV. DISCUSSION AND SUMMARY

The success of NCQ scaling of elliptic flow at  $\sqrt{s_{NN}}=200$  GeV has been one of the most striking observations at RHIC, strongly suggesting the creation of a flowing, thermalized bulk system of quarks that coalesce into hadrons. Hence, observing the violation of this scaling as  $\sqrt{s_{NN}}$  is decreased could be of crucial importance, both for validating the simple dynamical constituent quark model, and for pinpointing the conditions required to undergo the deconfinement phase transition. Furthermore, recent theoretical predictions suggest that a chiral magnetic wave effect may reveal itself by inducing a different flow for positive and negative pions [22]. The observation of NCQ scaling violations would thus be potentially far-reaching.

It is important, therefore, to explore less exotic reasons for any scaling violations. We have discussed one simple scenario here, which requires neither a fundamental difference in the

phase of QCD matter in the measured energy range, nor a new exotic effect.

The model predicts an unavoidable species-dependent pattern for the breakdown of NCQ scaling and depends on only two assumptions. Firstly, it assumes that, just as at top RHIC energies, the system can be described in terms of constituent quarks that coalesce into hadrons as the system cools. Secondly, it assumes that quarks transported from beam rapidity to midrapidity suffer more violent scatterings than do quarks produced at midrapidity at low  $\sqrt{s_{NN}}$ . We *simplified* the situation by treating the system as two distinct quark populations, but our main points do not depend on this simplification.

(Baryon transport from the entrance channel is another important ingredient of the model, but its relevance is far from an assumption; the phenomenon of stopping is well known and the isospin effect ( $X_{dT} > X_{uT}$ ) is obvious and based on data, as discussed in section II.)

The second of our two assumptions seems at least very plausible. It is clear that at low energies, the system does not have sufficient density or energy to fully thermalize— the dynamical constituents do not scatter enough. Unlike the produced particles born at midrapidity, however, the transported quarks had to undergo several collisions just to reach midrapidity, after which they could rescatter further.

It is the first assumption— that even at low energies where scaling violations might be found, the system is well-described by a flowing system of constituent quarks— that seems most questionable. Nevertheless, our task has been to explore the implications of its validity even at low  $\sqrt{s_{NN}}$ . We have found an unambiguous species dependence of  $v_2$  listed in equations 9. Quantitative details depend on tuning which we do not consider in this first study. Detailed comparisons with experimental data should be performed, but we have shown that violation of NCQ scaling or particle-antiparticle  $v_2$  degeneracy themselves is insufficient to claim either the crossing of the deconfinement threshold or exotic phenomena.

### Acknowledgements

We would like to thank Dr. Michael Mitrovski and Dr. Rosi Reed for helpful discussions. This work supported by the U.S. National Science Foundation under Grant PHY-0970048 and by the Offices of NP and HEP within the U.S. DOE Office of Science under the contracts DE-FG02-88ER40412 and DE-AC02-98CH10886.

- 
- [1] F. E. Taylor et al., Phys. Rev. **D14**, 1217 (1976).
  - [2] S. S. Adler et al. (PHENIX), Phys. Rev. Lett. **91**, 172301 (2003), nucl-ex/0305036.
  - [3] J. Adams et al. (STAR), Phys. Rev. Lett. **92**, 052302 (2004), nucl-ex/0306007.
  - [4] J. I. Kapusta, Phys. Rev. **C21**, 1301 (1980).
  - [5] H. Sato and K. Yazaki, Phys. Lett. **B98**, 153 (1981).
  - [6] J. L. Nagle, B. S. Kumar, D. Kusnezov, H. Sorge, and R. Mattiello, Phys. Rev. **C53**, 367 (1996).
  - [7] K. P. Das and R. C. Hwa, Phys. Lett. **B68**, 459 (1977).
  - [8] S. A. Voloshin, Nucl. Phys. **A715**, 379 (2003), nucl-ex/0210014.
  - [9] R. C. Hwa and C. B. Yang, Phys. Rev. **C67**, 064902 (2003), nucl-th/0302006.
  - [10] R. J. Fries, B. Muller, C. Nonaka, and S. A. Bass, Phys. Rev. Lett. **90**, 202303 (2003), nucl-th/0301087.
  - [11] V. Greco, C. M. Ko, and P. Levai, Phys. Rev. Lett. **90**, 202302 (2003), nucl-th/0301093.
  - [12] R. J. Fries, V. Greco, and P. Sorensen, Ann.Rev.Nucl.Part.Sci. **58**, 177 (2008), 0807.4939.
  - [13] B. Muller, R. J. Fries, and S. A. Bass, Phys. Lett. **B618**, 77 (2005), nucl-th/0503003.
  - [14] P. Sorensen (STAR), J. Phys. **G30**, S217 (2004), nucl-ex/0305008.
  - [15] P. Sorensen (2009), 0905.0174.
  - [16] M. S. Bhagwat, I. C. Cloet, and C. D. Roberts (2007), 0710.2059.
  - [17] L. Chang and C. D. Roberts (2010), 1003.5006.
  - [18] L. Ravagli and R. Rapp, Phys. Lett. **B655**, 126 (2007), 0705.0021.
  - [19] D. Krieg and M. Bleicher, Phys. Rev. **C78**, 054903 (2008), 0708.3015.
  - [20] S. A. Voloshin, A. M. Poskanzer, and R. Snellings (2008), 0809.2949.
  - [21] M. M. Aggarwal et al. (STAR) (2010), 1007.2613.
  - [22] Y. Burnier, D. E. Kharzeev, J. Liao, and H.-U. Yee (2011), 1103.1307.
  - [23] I. C. Arsene et al. (BRAHMS), Phys. Lett. **B677**, 267 (2009), 0901.0872.
  - [24] J. Randrup and J. Cleymans, Phys. Rev. **C74**, 047901 (2006).
  - [25] H. Oeschler, J. Cleymans, K. Redlich, and S. Wheaton, PoS **CPOD2009**, 032 (2009), 0910.2128.
  - [26] T. Anticic, B. Baatar, D. Barna, J. Bartke, H. Beck, L. Betev, H. Bialkowska, C. Blume, M. Bogusz, B. Boimska, et al. (NA49 Collaboration), Phys. Rev. C **83**, 014901 (2011), URL <http://link.aps.org/doi/10.1103/PhysRevC.83.014901>.
  - [27] Full data compilation from these measurements may be found on the web at [https://edms.cern.ch/file/1075059/1/na49\\_compil.pdf](https://edms.cern.ch/file/1075059/1/na49_compil.pdf) (2010).
  - [28] S. Afanasiev et al. (The NA49 Collaboration), Phys.Rev. **C66**, 054902 (2002), nucl-ex/0205002.
  - [29] T. Anticic et al. (NA49 Collaboration), Phys.Rev. **C69**, 024902 (2004).
  - [30] C. Alt et al. (NA49 Collaboration), Phys.Rev. **C73**, 044910 (2006).
  - [31] C. Alt et al. (NA49 Collaboration), Phys.Rev. **C77**, 024903 (2008), 0710.0118.
  - [32] C. Alt et al. (NA49 Collaboration), Phys.Rev. **C78**, 034918 (2008), 0804.3770.
  - [33] C. Alt et al. (NA49 collaboration), Phys.Rev. **C78**, 044907 (2008), 0806.1937.
  - [34] C. Alt et al. (NA49), Phys. Rev. **C68**, 034903 (2003), nucl-ex/0303001.
  - [35] D. Kharzeev, private communication (2011).
  - [36] Z.-w. Lin and C. M. Ko, Phys. Rev. Lett. **89**, 202302 (2002),

nucl-th/0207014.